

Properties of light-emitting porous silicon photoetched in aqueous HF/FeCl₃ solution

Yan Kai Xu and Sadao Adachi^{a)}

Department of Electronic Engineering, Faculty of Engineering, Gunma University, Kiryu-shi, Gunma 376-8515, Japan

(Received 23 January 2007; accepted 14 March 2007; published online 18 May 2007)

The formation of yellow-light-emitting porous silicon (PSi) layers in a HF solution with adding an oxidizing agent FeCl₃ is presented. The PSi layers are formed by photoetching under Xe lamp illumination. The photoluminescence (PL) intensity is strongly dependent on the FeCl₃ concentration and shows a maximum at $x \sim 25$ wt % [50 wt % HF: (x wt % FeCl₃ in H₂O)=1:1]. The surface topography as characterized by atomic force microscopy reveals features on the order of 20–100 nm with a root-mean-squares roughness of ≤ 2 nm. The Fourier-transform infrared spectroscopy shows a new absorption peak at ~ 1100 cm⁻¹, which is assigned to the surface oxide stretching mode and grows larger with increasing etching time. The stain etched samples also show PL emission, but they are synthesized only at higher x concentrations (≥ 20 wt %). The PSi formation mechanism can be explained with the aid of a surface energy-band diagram of n -type silicon in the HF/FeCl₃ electrolyte. © 2007 American Institute of Physics.

[DOI: 10.1063/1.2733752]

I. INTRODUCTION

Visible light emission from porous silicon (PSi) observed at room temperature has provoked a sustained search for its potential application in silicon-based optoelectronic devices and its academic interest.^{1,2} Such luminescent PSi layers are commonly formed by anodic etching on p -type silicon substrates. The first report of a luminescent porous layer obtained without electrochemical anodization came from Sarathy *et al.*³ who used a stain etching in a HF/HNO₃ solution. Noguchi and Suemune⁴ demonstrated the formation of a luminescent PSi spot by photoetching in a HF solution under He-Ne laser illumination for ~ 60 min. Subsequently, Yamamoto and Takai used a mixture of HF/H₂O₂ to obtain efficient PSi in short He-Ne illumination time (~ 10 – 30 min).^{5,6} More recently, Koker and Kolasinski⁷ used the circular-pattern radius produced by a 15 mW He-Ne laser to measure the photoetching rate of n -type Si(111) in various fluoride solutions. They also investigated the etching mechanisms of n - and p -type Si(111) in aqueous HF solutions under a continuous wave or a pulse laser irradiation of wavelengths 365, 473, 532, 633, 685, and 730 nm.⁸

In this article we report on a simple fabrication method of luminescent PSi layers on n -type silicon substrates. The PSi layer is formed by photoetching in a HF/FeCl₃ solution under Xe lamp illumination. The use of a Xe lamp enables a formation of large, homogeneous PSi layers. The addition of oxidant FeCl₃ in HF results in a stable formation of PSi layers in very short time. Properties of the photoetched PSi layers are characterized using photoluminescence (PL), atomic force microscopy (AFM), and Fourier-transform infrared spectroscopy (FTIR).

II. EXPERIMENT

Figure 1 shows an experimental arrangement used for the PSi formation by photoetching in a HF/FeCl₃ solution. The silicon substrates used were n -type Si(100) with a resistivity range of 1–3 Ω cm. They were degreased using organic solvents, followed by oxide removal with 50% HF solution, and then rinsed in de-ionized water.

Photoetching was performed at room temperature in an ultrasonic bath. The sample surface was illuminated by a 300 W Xe lamp through an optical filter blocking wavelengths shorter than 0.6 μ m. The chemical etchant used was 50 wt % HF solution adding an oxidizing agent of FeCl₃ x in wt % in H₂O [50 wt % HF: (x wt % FeCl₃ in H₂O)=1:1 in volume ratio]. After photoetching, the samples were rinsed in de-ionized water. The thickness of the PSi film was measured using a Talystep profilometer after a part of the film was removed by 2% NaOH solution.

PL measurements were performed using a grating spectrometer and a Peltier-device-cooled photomultiplier tube

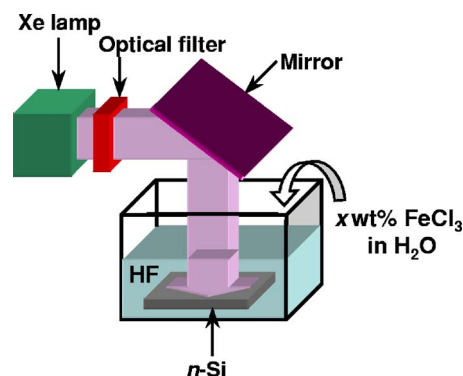


FIG. 1. (Color online) Experimental apparatus used for PSi formation by photoetching in a HF/FeCl₃ solution. Photoetching was performed under Xe lamp illumination through an optical filter cutting lights of $\lambda \leq 0.6$ μ m.

^{a)}Electronic mail: adachi@el.gunma-u.ac.jp

TABLE I. PL intensity for samples formed by stain and photoetching in solutions with adding an oxidizing agent of FeCl_3 x in wt % in H_2O [50 wt % HF:(x wt % FeCl_3 in H_2O)=1:1 in volume ratio].

Etching	x wt % FeCl_3 in H_2O			
	10	15	23	47
Stain	No emission	No emission	Very weak	Weak
Photoetching	Weak	Moderate	Strong	Weak

(Hamamatsu R375). The 325 nm line of a He–Cd laser (Kimmon IK3302R-E) chopped at 329 Hz was used as the excitation light source. The surface morphology of PSi sample was investigated by *ex situ* AFM, using a Digital Instruments Nanoscope III in the tapping mode and in the repulsive force regime. The surface chemistry of the PSi samples was monitored by FTIR. The FTIR spectra were recorded using a Nicolet Magna 560 spectrometer in the 400–2000 cm^{-1} region with a resolution of 4 cm^{-1} .

III. RESULTS AND DISCUSSION

A. Photoluminescence

We first discuss the effect of the FeCl_3 concentration on the PL emission intensity. The FeCl_3 concentration was varied from $x=10$ to 47 wt % in the 50 wt % HF solution. The samples were immersed in each solution for $t=1$ min with and without Xe lamp illumination. The results of these experiments are summarized in Table I. The corresponding surface morphologies observed by optical microscopy are shown in Fig. 2. It is well known that aqueous HF solution does not attack silicon harshly, but etches SiO_2 rapidly. The

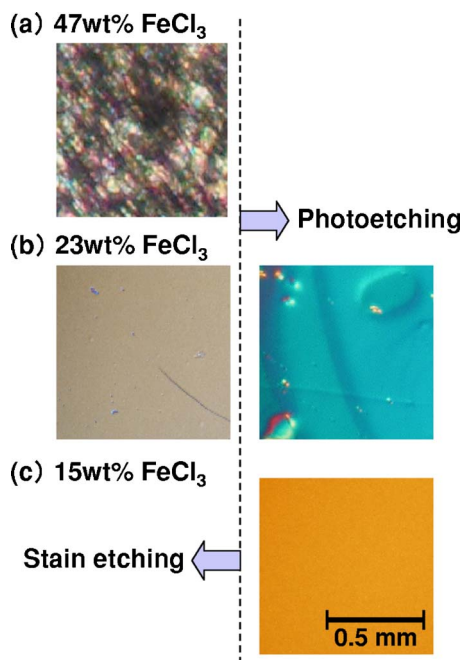


FIG. 2. (Color online) Surface view of n -type silicon samples observed by an optical microscopy ($\times 100$). (a) Stain etched in HF/ FeCl_3 solution with $x=47$ wt % ($t=1$ min), (b) stain and photoetched in HF/ FeCl_3 solution with $x=23$ wt % ($t=1$ min), and (c) photoetched in HF/ FeCl_3 solution with $x=15$ wt % ($t=3$ min).

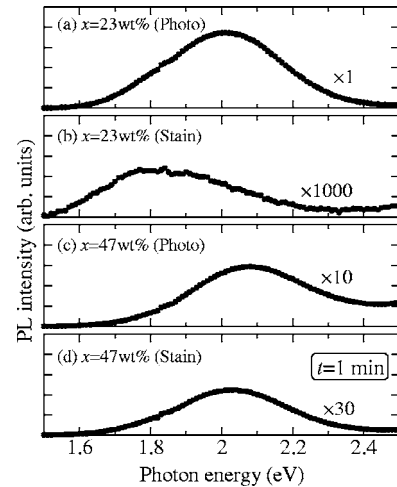


FIG. 3. PL spectra of PSi photoetched in HF/ FeCl_3 solutions with $x=23$ wt % and 47 wt % for $t=1$ min, together with those obtained by stain etching in the same solutions for $t=1$ min.

addition of a sufficient quantity of an oxidizing agent may lead to the oxidation of the silicon surface, resulting in silicon etching. More highly concentrated FeCl_3 may thus lead to more vigorous etching of the silicon substrate.

We can see in Table I that the sample etched at $x \leq 15$ wt % without Xe lamp illumination (stain etching) does not show PL emission. On the other hand, the samples photoetched in the $x=10$ –47 wt % solutions show PL emission and their intensity becomes maximum at $x=23$ wt % solution. We, however, found that large and homogeneous PSi layers can be more easily formed by photoetching in the $x=15$ wt % solution than in the 23 wt % solution [cf. Figs. 2(b) and 2(c)]. Thus, the results presented in the following are mainly obtained by photoetching in the $x=15$ wt % solution. It should also be noted that the sample etched in the high FeCl_3 ($x=47$ wt %) solution provides heavily stained surface morphology [Fig. 2(a)].

The room-temperature PL spectra of PSi photoetched in HF/ FeCl_3 solutions with $x=23$ wt % and 47 wt % for $t=1$ min, together with those obtained by stain etching in the same solutions for $t=1$ min are shown in Fig. 3. Note that the high energy tails seen in Figs. 3(b) and 3(c) come from the exciting light source (He–Cd laser). It is found that the photoetched PSi spectra [Figs. 3(a) and 3(c)] exhibit a broad emission peaking at ~ 2.0 – 2.1 eV, which is typically observed in stain etched PSi samples in HF/ HNO_3 -based solutions.^{3,9–14} The stain etched sample in the 47 wt % solution [Fig. 3(d)] also exhibits a broad peak at ~ 2 eV. On the other hand, the very weak PL emission from the stain etched sample in the 47 wt % solution [Fig. 3(b)] shows a broad peak at ~ 1.8 eV, which is typically observed in anodic PSi samples in HF/alcohol-based solutions.^{1,2,15–18}

Figure 4(a) plots the PL intensity versus photoetching time t for PSi formed in a HF/ FeCl_3 solution with $x=15$ wt %. It is seen that the PL intensity increases with increasing t and shows a saturation at $t \sim 2$ min. Note that the PSi formation time $t \sim 2$ min is much shorter than those formed in pure HF or a mixture of HF/ H_2O_2 ($t \sim 10$ – 30 min) using a coherent light source (He–Ne laser).^{4–6}

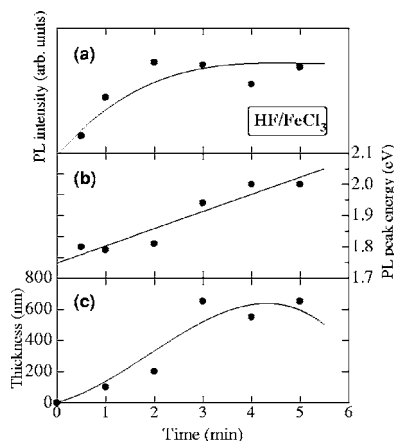


FIG. 4. Etching time dependence of (a) PL emission intensity, (b) PL peak energy, and (c) porous layer thickness formed in HF/FeCl₃ solution ($x = 15$ wt %).

The PL peak energy versus immersion time t in a HF/FeCl₃ solution is shown in Fig. 4(b). A gradual increase in the peak energy from ~ 1.8 to 2.0 eV is observed. Trends similar to those obtained here were observed in anodic PSi,^{19,20} where an energy shift from ~ 1.7 up to ~ 2.1 eV with prolonged anodization time was reported. PL spectra collected from our samples also show a peak width that is relatively invariant about 0.4 eV (see Fig. 3).

Figure 4(c) plots the PSi film thickness, determined by a Talystep profiler, versus immersion time t in a HF/FeCl₃ solution. The PSi thickness gradually increases with increasing t and shows a saturated value at $t \sim 3$ min. Unlike the anodic technique,²¹ we can see that the film thickness has a limited value, ~ 600 nm, which may be determined by several factors, such as the solution composition and temperature. In stained PSi,⁹ the limited thickness value is determined by the balancing of the silicon dissolution rates of the bottom part and the top surface of the porous layer. It is considered that the essentially same mechanism may occur during porous layer formation in photoetching as in stain etching.²² The PL intensity is also found to be roughly proportional to the PSi film thickness [cf. Figs. 4(a) and 4(c)].

B. Atomic force microscopy

To study surface properties of the PSi samples photoetched in HF/FeCl₃ solution, we used *ex situ* AFM. In Fig. 5, we show large-scale AFM images of the PSi samples photoetched in a HF/FeCl₃ solution with (a) $x = 15$ wt % for $t = 3$ min and (b) $x = 15$ wt % for $t = 5$ min, together with that obtained by stain etching in (c) $x = 47$ wt % solution for $t = 1$ min.

In Fig. 5(a), the AFM image reveals many irregularly shaped hillocks and voids distributed randomly over the entire surface. The root-mean-square (rms) roughness obtained from this image is ~ 1.0 nm. The lateral microstructures observed are on the order of 20–100 nm. In Fig. 5(b), many elongated oval shapes can be found and their lateral sizes are much larger than those in Fig. 5(a). The rms roughness in Fig. 5(b) is ~ 2.4 nm. We also observed AFM images from samples photoetched in the 15 wt % solution for $t = 0.5$ and 1

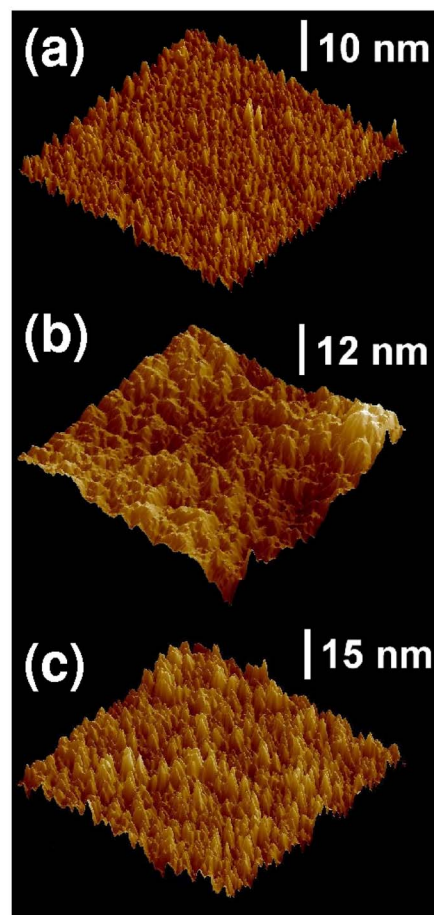


FIG. 5. (Color online) Large-scale ($1 \mu\text{m} \times 1 \mu\text{m}$) AFM images of the PSi samples photoetched in HF/FeCl₃ solution with (a) $x = 15$ wt % for $t = 3$ min and (b) $x = 15$ wt % for $t = 5$ min, together with that obtained by stain etching in (c) $x = 47$ wt % solution for $t = 1$ min.

min. The corresponding rms roughness is 0.6 ($t = 0.5$ min) and 0.8 nm (1 min). It is thus considered that the rms roughness increases with increasing photoetching time t . The stain etched sample [Fig. 5(c)] shows AMF figures that are essentially the same as seen in Fig. 5(b). The rms roughness obtained from Fig. 5(c) is ~ 2.0 nm, slightly smaller than that in Fig. 5(b).

If the porous size is truly on the order of 20–100 nm, the electronic states in such macroscopic pores are not quantum confined. We must note, however, that the nanocrystalline sizes in the walls of the pores are important for quantum confinement effects. The nanocrystalline size may be related to the thickness of the pore walls, but not to the lateral pore size. Due to tip convolution, an accurate nanocrystalline size determination is impossible in AFM measurement. For stained PSi samples,⁸ the dimensions of most pits were reported to be in the range of ~ 200 –400 nm, which are much larger than the sizes required to induce quantum confinement effects, but the stained samples emitted visible lights. Recently, we carried out scanning electron microscopy measurements on stain etched PSi in a HF/K₂Cr₂O₇ solution and observed nanocrystalline lumps of less than 10 nm on the macroscopic pores.

AFM and transmission electron microscopy images showed that the anodized and stained PSi showed a “fractal-

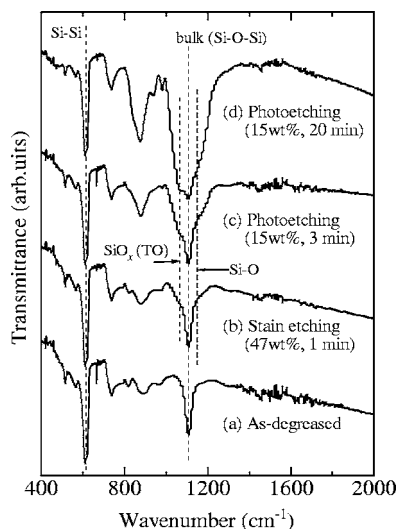


FIG. 6. FTIR spectra of (a) as-degreased crystalline silicon, (b) HF/FeCl₃-prepared PSi by stain etching (47 wt %, 1 min), (c) HF/FeCl₃-prepared PSi by photoetching (15 wt %, 3 min), and (d) HF/FeCl₃-prepared PSi by photoetching (15 wt %, 20 min).

type” surface morphology.²³ It is, thus, possible to consider that the nanocrystalline silicon enables the nondirect optical transition via a relaxation of the momentum conservation at energies well above the indirect-absorption edge, resulting in a supraband gap (E_g^X) emission in the visible spectrum region. Such a supraband gap emission has been clearly observed in porous GaP.²⁴

C. Fourier-transform infrared spectroscopy

To further survey the origin of the visible emission in the HF/FeCl₃-prepared PSi, we performed FTIR measurements at room temperature. Figure 6 shows FTIR spectra of (a) as-degreased crystalline silicon, (b) HF/FeCl₃-prepared PSi by stain etching (47 wt %, 1 min), (c) HF/FeCl₃-prepared PSi by photoetching (15 wt %, 3 min), and (d) HF/FeCl₃-prepared PSi by photoetching (15 wt %, 20 min).

The FTIR spectrum of the as-degreased crystalline silicon [Fig. 6(a)] exhibits strong absorption peak near 614 cm⁻¹. This peak is due to the lattice absorption band (Si-Si). The peak at ~1107 cm⁻¹ can be assigned to the bulk Si-O-Si mode. Weak absorption shoulders are observed at ~1067 and ~1150 cm⁻¹ in the stain etched PSi sample [Fig. 6(b)]. These absorptions grow large as photoetching time increases in the 15 wt % solution [Figs. 6(c) and 6(d)]. The absorptions at ~1067 and ~1150 cm⁻¹ are assigned to the transverse optical phonons in thin SiO_x layer and to the Si-O stretching mode, respectively.²⁵

It is noted that the PSi samples passively etched in HF solution still emitted light in the visible region, but its strength becomes very weak. We, therefore, consider that the light emission observed in the HF/FeCl₃-prepared PSi sample is not arising from any oxide or its related centers. It is suggested that the surface oxide acts as a good passivation film and gives rise to an efficient emission at the PSi/oxide interface.^{26,27} We must note, however, that the surface of freshly etched PSi is almost totally covered by SiH_x groups. It has been reported that it is difficult to establish a direct

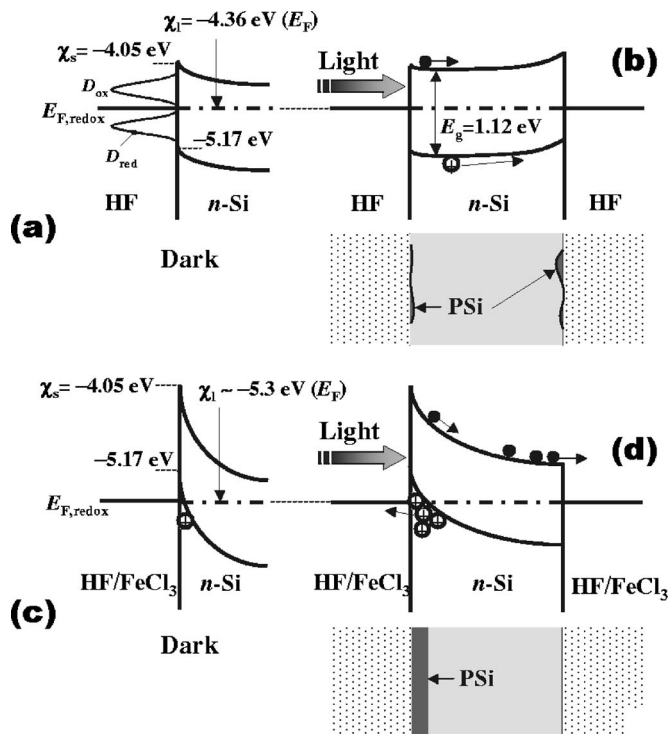


FIG. 7. Energy-band diagrams for *n*-Si immersed in pure HF solution [(a) and (b)] and those in HF/FeCl₃ solution [(c) and (d)]. In (b), PSi is formed stably on the backside in opposition to the illuminated surface. In (d), PSi is formed on the illuminated surface.

correlation between the visible luminescence properties in PSi and any particular chemical species, such as hydrides, oxide, or siloxene.²⁸

We finally present in Fig. 7 the schematic energy-band diagrams for *n*-Si electrodes in pure HF (*pH*=2.3) and HF/FeCl₃ solutions without and with light illumination.^{29,30} The electron affinity χ_s for silicon is -4.05 eV.³¹ The pure HF solution has a *pH* value of 2.3. Then, the electron energy of the pure HF solution with respect to vacuum is -4.36 eV (χ_l).³² After immersion of the silicon substrate into the electrolyte in the dark, the Fermi levels E_F and $E_{F,redox}$ on both sides of the *n*-Si/electrolyte interface are brought to be the same energy level by a transfer of electrons from the silicon substrate into the electrolyte [Fig. 7(a)].

The half-reaction for oxidizing agent FeCl₃ is³³

$$\text{Fe}^{3+} + e^- = \text{Fe}^{2+} \quad (E^o = 0.771 \text{ V}), \quad (1)$$

where e^- represents the electron and E^o is the standard reduction potential in respect to the standard hydrogen electrode. Then, the redox potential E_{abs} on the vacuum scale of the HF/FeCl₃ redox system is then given by

$$E_{abs} = -4.5 - E^o \sim -5.3 \text{ eV}. \quad (2)$$

Note that the larger the E^o value in the positive (negative) sign, the stronger the oxidation (reduction) agent. It is thus understood that the HF/FeCl₃ solution is more oxidative than the HF solution. The corresponding energy-band scheme is schematically shown in Fig. 7(c).

The energy-band diagrams shown in Figs. 7(a) and 7(c) have some similarities to that of the Schottky contact characterized by a metal/semiconductor interface. The photoex-

cited electrons and holes are separated by the electric field in the surface space-charge layer, with the electrons and holes drifting into the opposite directions. The holes at the electrolyte/*n*-Si interface can participate in PSi formation. In Fig. 7(b), however, the photoexcited holes can suffer to drift toward the surface due to the very small downward band bending or, possibly, due to the nearly flatband. Thus, no efficient PSi formation can be expected in the pure HF solution. If wafer is dipped in the HF/FeCl₃ solution [Fig. 7(d)], on the other hand, a large number of photoexcited holes move toward the electrolyte/*n*-Si interface at the front surface, resulting in the formation of PSi with good reproducibility. The electrons arrived at the backsurface can be used in the reduction of FeCl₃. This should be the main reason that the PSi formation is accelerated in the existence of FeCl₃ in the HF solution. The effects of adding oxidizing agents, including FeCl₃, in various fluoride solutions on the kinetics of PSi formation with and without light illumination have been discussed in more detail in Refs. 7 and 8.

Andersen *et al.*³⁴ suggested that the preexisting state of the silicon surface plays a decisive role in determining PSi formation. They reported that cleaning the samples with organic solvents prior to treating then with HF did not improve the outcome, but pretreating a sample with aqueous KOH solution resulted in formation of PSi during the subsequent treatment with HF combined with He–Ne laser illumination. However, no PSi layer was observed for samples treated less than 1 h in KOH. In all cases, the PSi spot on the front surface showed poor or no PL. Surprisingly enough, however, the PSi was formed on that surface of the sample, which was not exposed with illumination, i.e., on the backside. On the backside of all samples treated ≥ 1 h in KOH, a dark spot became visible and increased its size with increasing time in KOH. Uniform visible PL was observed from all of the spots on the backsurface.³⁴

More recently, Koker and Kolasinski⁸ suggested that hydrocarbon contamination is one contributor to this type of abnormality. They found that through cleaning of the silicon wafer as well as the apparatus with methanol and acetone in an ultrasonic bath minimizes the variability. The PSi formation rate increased if the silicon wafer is left in aqueous HF solution for extended periods prior to light irradiation. This was particularly noticeable in 48% HF solution for which it took ~ 1 h to reach a steady-state rate. They also suggested that the acceleration may be due to chemical etching of the silicon surface which causes surface microroughening.⁸

The HF/electrolyte/*n*-Si energy scheme in Fig. 7(b) can successfully explain why PSi is sometimes formed on the backside in opposition to the illuminated surface, as was observed by Andersen *et al.*³⁴ In the HF/FeCl₃-electrolyte/*n*-Si scheme, the energy bands of *n*-Si are strongly bent downward, as shown in Fig. 7(c). By illuminating light, the electrons and holes are generated in *n*-Si [Fig. 7(d)]. Since an electric field exists across the space charge region at the electrolyte/*n*-Si interface, the electrons and holes are separated. Then, potentials across the space charge, and consequently the band bending, are reduced. A “large” number of

holes accumulated at the HF/FeCl₃-electrolyte/*n*-Si interface can be participated in forming PSi layer only on the front surface [Fig. 7(d)].

IV. CONCLUSIONS

It was shown that large PSi layers can be synthesized on *n*-type silicon by photoetching in HF solution with adding FeCl₃ under Xe lamp illumination. The addition of FeCl₃ into HF largely shortened PSi formation time from ~ 10 – 60 min to a few minutes. The PL spectra exhibited a broad peak at ~ 2.0 eV. The AFM image revealed many irregularly shaped pores and voids distributed randomly over the entire surface at shorter etching times and elongated oval shapes at longer times. The FTIR spectroscopy showed an appearance of the surface Si–O–Si stretching mode $\nu(\text{Si}–\text{O}–\text{Si})$ at ~ 1064 cm⁻¹. This surface oxide was expected to act as a good passivation film and gives rise to an efficient emission at the PSi/oxide interface. The PSi formation mechanism could be simply explained with the aid of surface energy-band diagram of *n*-type silicon in the HF/FeCl₃ electrolyte.

ACKNOWLEDGMENTS

The authors would like to thank Professor T. Miyazaki and Professor S. Ozaki and S. Kido, K. Inoue, and S. Sozawa for their experimental support and useful discussion. This work was supported in part by the Foundation for Technological Promotion of Electronic Circuit Board.

- ¹A. G. Cullis, L. T. Canham, and P. D. J. Calcott, *J. Appl. Phys.* **82**, 909 (1997).
- ²S. Ossicini, L. Pavesi, and F. Priolo, *Light Emitting Silicon for Microphotonics* (Springer, Berlin, 2003).
- ³J. Sarathy *et al.*, *Appl. Phys. Lett.* **60**, 1532 (1992).
- ⁴N. Noguchi and I. Suemune, *Appl. Phys. Lett.* **62**, 1429 (1993).
- ⁵N. Yamamoto and H. Takai, *Jpn. J. Appl. Phys.*, Part 1 **38**, 5706 (1999).
- ⁶N. Yamamoto and H. Takai, *Thin Solid Films* **359**, 184 (2000).
- ⁷L. Koker and K. W. Kolasinski, *J. Phys. Chem. B* **105**, 3864 (2001).
- ⁸L. Koker and K. W. Kolasinski, *Phys. Chem. Chem. Phys.* **2**, 277 (2000).
- ⁹S. Shih, K. H. Jung, T. Y. Hsieh, J. Sarathy, J. C. Campbell, and D. L. Kwong, *Appl. Phys. Lett.* **60**, 1863 (1992).
- ¹⁰J. L. Coffer, S. C. Lilley, R. A. Martin, and L. A. Files-Sesler, *J. Appl. Phys.* **74**, 2094 (1993).
- ¹¹M. T. Kelly, J. K. M. Chun, and A. B. Bocarsly, *Appl. Phys. Lett.* **64**, 1693 (1994).
- ¹²Ş. Kalem and M. Rosenbauer, *Appl. Phys. Lett.* **67**, 2551 (1995).
- ¹³M. J. Winton, S. D. Russell, J. A. Wolk, and R. Gronsky, *Appl. Phys. Lett.* **69**, 4026 (1996).
- ¹⁴M. Nahidi and K. W. Kolasinski, *J. Electrochem. Soc.* **153**, C19 (2006).
- ¹⁵V. Petrova-Koch, T. Muschik, A. Kux, B. K. Meyer, and F. Koch, *Appl. Phys. Lett.* **61**, 943 (1992).
- ¹⁶T. Maruyama and S. Ohtani, *Appl. Phys. Lett.* **65**, 1346 (1994).
- ¹⁷B. R. Mehta, M. K. Sahay, L. K. Malhotra, D. K. Avasthi, and R. K. Soni, *Thin Solid Films* **289**, 95 (1996).
- ¹⁸D. W. Cooke, R. E. Muenchausen, B. L. Bennett, L. G. Jacobsohn, and M. Nastasi, *J. Appl. Phys.* **96**, 197 (2004).
- ¹⁹C. Peng, L. Tsybeskov, and P. M. Fauchet, *Mater. Res. Soc. Symp. Proc.* **283**, 121 (1993).
- ²⁰M. B. Robinson, A. C. Dillon, and S. M. George, *Mater. Res. Soc. Symp. Proc.* **283**, 191 (1993).
- ²¹P. C. Searson, *Appl. Phys. Lett.* **59**, 832 (1991).
- ²²T. Hadjersi, E. S. Kooij, N. Yamamoto, K. Sakamaki, H. Takai, and N. Gabouze, *Phys. Status Solidi C* **2**, 3375 (2005).
- ²³T. George, M. S. Anderson, W. T. Pike, T. L. Lin, R. W. Fathauer, K. H. Jung, and D. L. Kwong, *Appl. Phys. Lett.* **60**, 2359 (1992).

- ²⁴K. Tomioka and S. Adachi, *J. Appl. Phys.* **98**, 073511 (2005).
- ²⁵M. Saadoun, B. Bessais, N. Mliki, M. Ferid, H. Ezzaouia, and R. Benna-ceur, *Appl. Surf. Sci.* **210**, 240 (2003).
- ²⁶K. Tsunoda, E. Ohashi, and S. Adachi, *J. Appl. Phys.* **94**, 5613 (2003).
- ²⁷T. Maruyama and S. Ohtani, *Appl. Phys. Lett.* **65**, 1346 (1994).
- ²⁸S. Banerjee, K. L. Narasimhan, and A. Sardesai, *Phys. Rev. B* **49**, 2915 (1994).
- ²⁹R. Memming, in *Comprehensive Treatise of Electrochemistry*, edited by B. E. Conway, J. O'M. Bockris, E. Yeager, S. U. M. Khan, and R. E. White (Plenum, New York, 1983), Vol. 7, p. 529.
- ³⁰S. Adachi and T. Kubota, *Electrochem. Solid-State Lett.* **10**, H39 (2007).
- ³¹S. Adachi, *Properties of Group-IV, III-V and II-VI Semiconductors* (Wiley, Chichester, 2005).
- ³²H. Seidel, L. Csepregi, A. Heuberger, and H. Baumgärtel, *J. Electrochem. Soc.* **137**, 3612 (1990).
- ³³P. Vanýsek, in *CRC Handbook of Chemistry and Physics*, edited by D. R. Lide (CRC, Boca Raton, 2001), p. 8.
- ³⁴O. K. Andersen, T. Frello, and E. Veje, *J. Appl. Phys.* **78**, 6189 (1995).